Supporting Information

Carbon Supported Au_{25} Cluster Electrocatalyst Decorated with Dendron Thiolates: Enhanced Loading Weight and Durability for Hydrogen Evolution Reaction

Kosuke Sakamoto,[†] Shinya Masuda,[†] Shinjiro Takano,[†] and Tatsuya Tsukuda[*,†]

[†]Department of Chemistry, Graduate School of Science, The University of Tokyo, Hongo 7-3-1, Bunkyo-Ku, Tokyo 113-0033, Japan

Corresponding Author

**E-mail: tsukuda@chem.s.u-tokyo.ac.jp*

1. Experimental

1.1 Chemicals

Hydrogen tetrachloroaurate (III) tetrahydrate ($HAuCl_4 \cdot 4H_2O$) was purchased from Tanaka Precious Metals. Sodium borohydride ($NaBH_4$), silica for column chromatography (SiO_2), sulfuric acid (H_2SO_4), sodium hydroxide (NaOH), potassium hydroxide (KOH), benzyl alcohol ($PhCH_2OH$), hydrochloric acid (HCl), sodium chloride (NaCl), anhydrous magnesium sulfate ($MgSO_4$), 5% Nafion® Dispersion Solution DE521 CS type (Nafion), methanol (MeOH), ethanol (EtOH), dichloromethane (DCM), *n*-hexane, toluene, and 2-propanol were purchased from FUJIFILM Wako Pure Chemical Industries. Tetrahydrofuran (THF; anhydrous, stabilizer-free) was purchased from Kanto Chemicals. Acetonitrile (MeCN) and tetraoctylammonium bromide (TOAB) were purchased from Sigma-Aldrich. 2-Phenylethanethiol (PET-H), 3,5-bis[3,5-bis(benzyloxy)benzyloxy]benzyloxy bromide (D2Br), thiourea, and *trans*-2-[3-(4-*tert*-butylphenyl)-2-methyl-2-propenylidene]malononitrile (DCTB) were purchased from Tokyo Chemical Industry. Porous carbon support (CNovel, grade: P(3)010-00) was purchased from Toyo Tanso. Milli-Q grade water (>18 MΩ cm) was used. All chemicals were used as purchased.

1.2 Characterization

Ultraviolet-visible (UV-Vis) absorption spectra were measured in the transmission mode using JASCO V-670 and V-630 spectrophotometers at room temperature with a quartz cuvette (1 cm × 1 cm). Gel permeation chromatography (GPC) was performed using a high-performance liquid chromatography (HPLC) system (LC-908, Japan Analytical Industry) equipped with a preparative GPC column (T30000, YMC Co., Ltd.). The mobile phase was toluene at a flow rate of 5.5 or 6.0 mL/min. The UV chromatogram was monitored at a wavelength of 300 nm. Typically, the crude mixture in toluene (20 mg/mL, <2.0 mL) was injected and recycled once before manual fractionation. The aliquot of each fraction was evaporated and dissolved in DCM, and UV-vis absorption spectra were measured to verify purity. Matrix-assisted laser desorption/ionization mass spectrometry (MALDI-MS) data were recorded using a SHIMADZU MALDI-8030 apparatus. Typically, MALDI-MS samples were prepared by dissolving $[Au_{25}(SR)_{18}]^0$ clusters (0.1 mg) and DCTB matrix (1.0 mg) in toluene (20 μL), and 1.0 μL of the mixed solution was dropped onto the MALDI plate. All the data

were collected in negative ion mode. Thermogravimetric analysis (TGA) was performed using a SII TG-DTA 7200 instrument (Hitachi High-Tech Science). The samples (~2.0 mg) were loaded on the aluminum pan and the data were collected under air at the flow rate of 50 mL/min. The temperature was raised from 20 °C to 500 °C at the rate of 1 °C /min and then held at 500 °C for 2 h. Powder X-ray diffraction (PXRD) patterns were collected using a diffractometer and D/teX Ultra 250 detector (SmartLab 3, Rigaku) with Cu Kα characteristic radiation (λ = 1.5405 Å). The measurement and analysis were performed using the SmartLab Studio II software (Rigaku). Aberration-corrected high-angle annular dark-field scanning transmission electron microscopy (AC-HAADF-STEM) images were obtained using a JEM-ARM200F microscope operated at 200 kV, under 1×10^{-5} Pa at 298 K in the sample column. The AC-HAADF-STEM samples were prepared by dropping the acetone dispersion of the catalysts onto copper grids (Okenshoji Co. Ltd Microgrid). The obtained AC-HAADF-STEM images were analyzed using the Fiji ImageJ program.[S1] Histograms were generated by counting at least 300 particles. Au L_3-edge X-ray absorption spectroscopy (XAS) was performed in transmission mode at room temperature using an ion chamber as a detector in the BL01B1 or BL14B2 beamlines at the SPring-8 of the Japan Synchrotron Radiation Research Institute (JASRI) (proposal: 2023A1635 and 2023B2004). The incident X-ray beam was monochromatized using a Si (111) double crystal monochromator. The X-ray energy was calibrated with an Au foil. The XAS samples were prepared by packing ~80 mg (1 wt%) or ~15 mg (5 wt%) of catalysts into the plastic cuvette (1 cm × 1 cm), which was pushed by an aluminum rod (1 cm × 1 cm). The data were analyzed using REX2000 software (Rigaku). The k^3-weighted χ spectra of EXAFS in the k range of 3.0-14.0 were Fourier transformed into r-space. Curve fitting analysis was performed for Au–S and Au–Au bonds in the range of 1.6-3.1 Å. X-ray photoelectron spectroscopy (XPS) measurement was performed using a PHI 5000 VersaProbe III instrument (ULVAC-PHI) with the Al Kα X-rays (1486.6 eV) at an energy resolution of 0.1 eV. The samples were prepared by mounting the catalysts on a carbon tape. The energy calibration was performed as follows. First, the peak of Au $4f_{7/2}$ of the Au foil was shifted to 84.0 eV and the energy shift was also applied to C 1s. The C 1s peak of the samples was adjusted to the same value.

1.3 Synthesis of D2S-H

The D2S-H ligand was synthesized according to the reported procedure with slight modifications.[S2] Typically, a test tube was charged with D2Br (1.0 mmol), thiourea (1.0 mmol), and a magnetic stirring bar. Shortly after adding EtOH/THF = 1:1 (v/v) (5 mL), the gas phase was replaced with pure Ar by ballooning and stirring was started at 80 °C. After 4 h, 1 M KOH*aq* (2 mL) was added to the reaction solution using a syringe and a needle, resulting in a white suspension. After further stirring at 80 °C under Ar for 4 h, the reaction solution was cooled to room temperature. 1 M HCl*aq* (4 mL) was added to the reaction solution using a syringe and a needle, followed by stirring under Ar for 10 min. The reaction solution was collected in an eggplant flask with DCM and was evaporated to remove organic solvents. The remaining aqueous layer was mixed three times with DCM to extract a crude product. The DCM layer was collected and evaporated to obtain an oily product. This oily product was washed by centrifugation with water three times and MeOH four times. The white solid of the title compound was dried *in vacuo* overnight. The yield was 92%.

1.4 Synthesis of 2-phenylethanethiolate protected Au cluster, $[Au_{25}(PET)_{18}]^0$

The title compound was synthesized according to the reported procedure with modifications.[S3] Typically, a 300 mL eggplant flask was charged with $HAuCl_4 \cdot 4H_2O$ (0.96 mmol), TOAB (1.1 mmol),

and a magnetic stirring bar. THF (52.5 mL) was added to the flask, and the color of the solution was changed to dark red after stirring for 15 min at room temperature in air. Then, 2-phenylethanethiol (9.5 mmol) was added dropwise to the solution and the stirring was continued for 2 h. The color of the solution gradually faded away during stirring. The freshly prepared, ice-cold $NaBH_4$ solution (9.6 mmol in 7.5 mL water) was added to the reaction solution all at once. The solution immediately turned dark brown with strong gas evolution. After stirring for 48 h, the reaction solution was filtered through a paper filter and the THF layer was collected. After evaporation, black oil covered with water was obtained. The oil was precipitated with methanol and the precipitate was washed by centrifugation. This methanol washing procedure was repeated at least five times, and the resulting precipitate was dried *in vacuo*. The dried product was extracted with a small amount of acetonitrile, followed by evaporation. The resulting precipitate was further purified by silica gel column chromatography with an eluent of *n*-hexane/DCM = 1.5:1 (v/v). The dark green band was collected and dried *in vacuo*. The product obtained was recrystallized in toluene by layering EtOH (toluene/EtOH = 1:10 (v/v), with the concentration of 20 mg/mL in toluene). The crystal was collected by filtration, washed with MeOH, and dried *in vacuo* to give the title compound. The yield was 16% based on Au.

1.5 Ligand exchange of $[Au_{25}(PET)_{18}]^0$ with D2S-H

A 25 mL eggplant flask was charged with the DCM solution of $[Au_{25}(PET)_{18}]^0$ (4.1 mM, 2 mL) and a magnetic stirring bar. DCM solution containing 5 or 20 equivalents of D2S-H with respect to $[Au_{25}(PET)_{18}]^0$ (20 or 80 mM for 5 or 20 equivalents, respectively, 2 mL) was added dropwise to the eggplant flask. After stirring the reaction solution for 12 h, MeOH was added to the solution and the DCM was evaporated. The MeOH suspension obtained was centrifuged to precipitate the ligand-exchanged products. The products obtained by addition of 5 or 20 equivalents of D2S-H were washed by centrifugation with DCM/*n*-hexane = 1:15 or 1:8 (v/v), respectively. In this washing procedure, the products were first dissolved in a small amount of DCM and then precipitated by adding a large amount of *n*-hexane. This washing procedure was repeated at least five times. After drying *in vacuo*, the products were extracted with toluene and further purified by GPC. The ligand exchanged products were obtained after evaporation and drying *in vacuo*. The compositions of the products were determined by MALDI-MS (Figure 1B) and TGA (Figure 1C). The average number of D2S introduced (x) was calculated from the MALDI mass spectra by fitting the ion intensity distribution with a Gaussian function. Yields were 49% and 90% for 5 and 20 equivalent samples, respectively (based on Au and the determined composition).

1.6 Preparation of supported Au cluster catalysts

The carbon supported Au cluster catalysts were prepared according to the reported procedure with modifications.[S4] Typically, a 300 mL Erlenmeyer flask was charged with CNovel (300 mg), toluene (100 mL), and a magnetic stirring bar. The CNovel was dispersed in toluene by sonication at room temperature for 30 min, followed by vigorous stirring at 0 °C for 30 min. Meanwhile, a toluene solution (100 mL) containing the calculated amount of $[Au_{25}(SR)_{18}]^0$ clusters (1.0 wt% based on the metal weight) was prepared, and the UV-vis absorption spectrum was measured to calculate the amount of cluster loading. The toluene solution was added dropwise at a rate of 1 mL/min. After 2 h of stirring at 0 °C, the composites were collected by filtration and were dried *in vacuo* for overnight. The filtrate was also collected and evaporated to measure the UV-vis absorption spectrum.

For the preparation of composites with a loading amount of 5.0 wt%, almost the same procedure was followed except that the amount of CNovel was reduced to 60 mg. The solution containing

clusters was prepared with the same concentration as in the case of 1.0 wt%.

The resulting composites (100 mg or 20 mg for 1.0 wt% or 5.0 wt%, respectively) on a quartz boat were then placed in a furnace and calcined under vacuum at a certain temperature (400 or 425 ℃). The calcination time at 400 ℃ was 12 h for 1.0 wt%, while that at 425 ℃ was 8, 12, 15, 18, 21, or 24 h for 1.0 wt% and 12, 15, 18, or 24 h for 5.0 wt%. The temperature was raised to 400 or 425 ℃ at a rate of 5 ℃/min and held at that temperature for the calcination time.

1.7 Preparation of supported Au nanoparticle catalyst (5.0 wt%)

A 200 mL eggplant flask was charged with CNovel (500 mg), acetone (50 mL), water (80 mL) and a magnetic stirring bar. The suspension was sonicated for 1 min before adding aqueous $HAuCl_4$ solution (40 mM, 3.34 mL). Aqueous ammonia solution (28%, 200 mL) was slowly added to adjust the pH to approximately 9. After stirring for 30 min, ice-cold $NaBH_4$ solution (0.40 mmol in 7.5 mL water) was added all at once to the suspension and kept under stirring for 30 min. The solid was collected by filtration and washed with water (500 mL) and acetone (50 mL), followed by drying *in vacuo* overnight.

1.8 Catalytic oxidation of benzyl alcohol

Catalytic oxidation of benzyl alcohol was performed using ChemiStation equipment (PPS-1510, EYELA). Typically, the test tube was filled with a magnetic stirring bar, 5.0 mg of samples, 1 mL each of aqueous benzyl alcohol (Au 0.33 mol%) and NaOH (300 mol%) solutions. The tube was immediately stirred at 30 ℃ and the gas phase was replaced with pure O_2 through a balloon. An excess amount of HCl (35%, 150 μL) was added to quench the reaction after 30 min. The substrates and products were extracted with toluene at least three times. To improve the extraction efficiency, an excess amount of NaCl was added during the extraction. The organic phase was collected and was dehydrated with anhydrous $MgSO_4$. The solids were removed through a syringe filter and the extract was diluted to 10 mL using a volumetric flask. The extract obtained was analyzed by gas chromatography (GC, GC-2025, Shimadzu) with a flame ionization detector.

1.9 Electrocatalytic hydrogen evolution reaction (HER)

The catalytic activities of HER were investigated using a BAS RRDE-3A rotating ring disk system with a rotation speed of 5000 rpm. An EC FRONTIER ECstat-400 potentiostat with a conventional three-electrode system was used. The working electrode (WE) was a glassy carbon rotating disk electrode (RDE) with φ = 3 mm; the counter electrode was a carbon rod; and the reference electrode was Ag/AgCl (in 3.5 M KCl solution). The potentials were calibrated to a reversible hydrogen electrode (RHE): $E_{RHE} = E_{Ag/AgCl} + 0.213$ (V). The value for calibration, 0.213 V, was measured under experimental condition with working electrode Ag/AgCl against RHE. The catalyst ink was prepared by dispersing the catalyst in a mixture of *n*-hexane, 2-propanol, and Nafion at a ratio of 4.5:4.5:1 to obtain 0.42 mg Au/mL. 17 μL of the ink was dropped onto the RDE and was dried for 2 h at ambient conditions. The electrolyte was 0.5 M H_2SO_4 and the temperature during the measurement was 30 ℃. Linear sweep voltammetry (LSV) was measured at a scan rate of 2 mV/s in the range from −0.1 V to −0.8 V vs. Ag/AgCl. Stability testing was performed by two methods: potential cycling and controlled potential electrolysis. For potential cycling, cyclic voltammetry (CV) was scanned in the range of −0.8 V ∼ −0.1 V vs. Ag/AgCl at a scan rate of 500 mV/s. LSV was then recorded after the determined number of cycles. For controlled potential electrolysis, a constant voltage of −0.6 V vs. Ag/AgCl was applied during the measurement and the current flow was recorded for 8 h.

2. Results

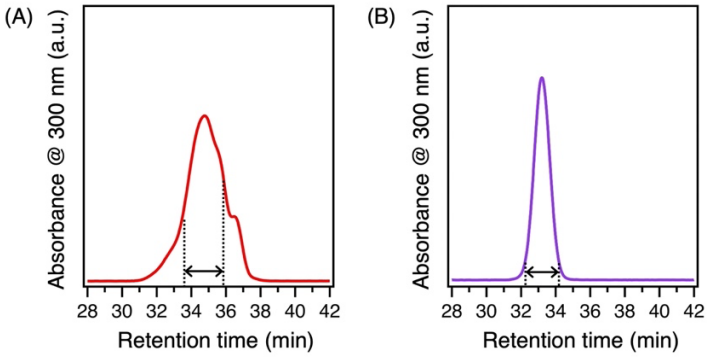

Figure S1. GPC charts of the ligand exchange products prepared by adding (A) 5 and (B) 20 equivalents of D2S-H to $[Au_{25}(PET)_{18}]^0$: the flow rate, 6.0 mL/min; eluent, toluene. The fractional components indicated by both arrows were used as purified samples.

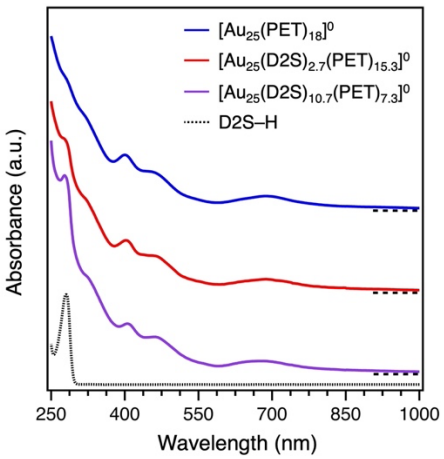

Figure S2. UV-Vis absorption spectra of $[Au_{25}(D2S)_x(PET)_{18-x}]^0$ prepared with 0 (blue), 5 (red), and 20 (purple) equivalents of D2S–H, respectively, and D2S–H (black, dotted) in DCM.

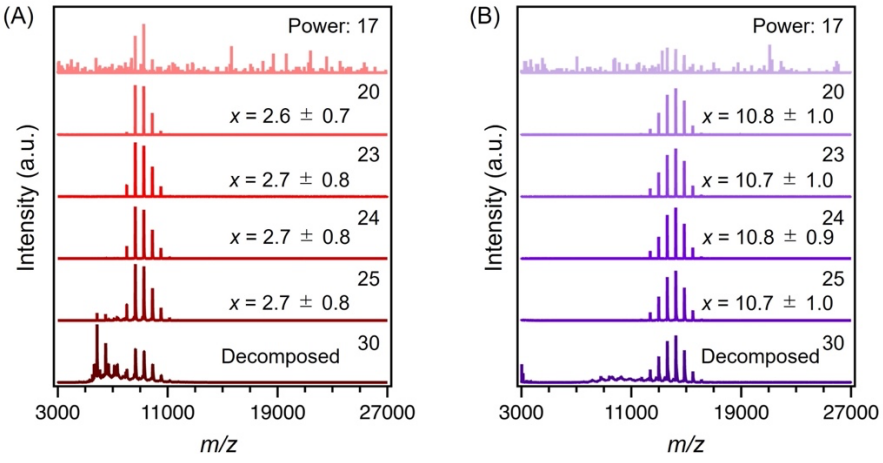

Figure S3. Negative-mode MALDI mass spectra of $[Au_{25}(D2S)_x(PET)_{18-x}]^0$ prepared with (A) 5 and (B) 20 equivalents of D2S–H recorded at different laser powers.

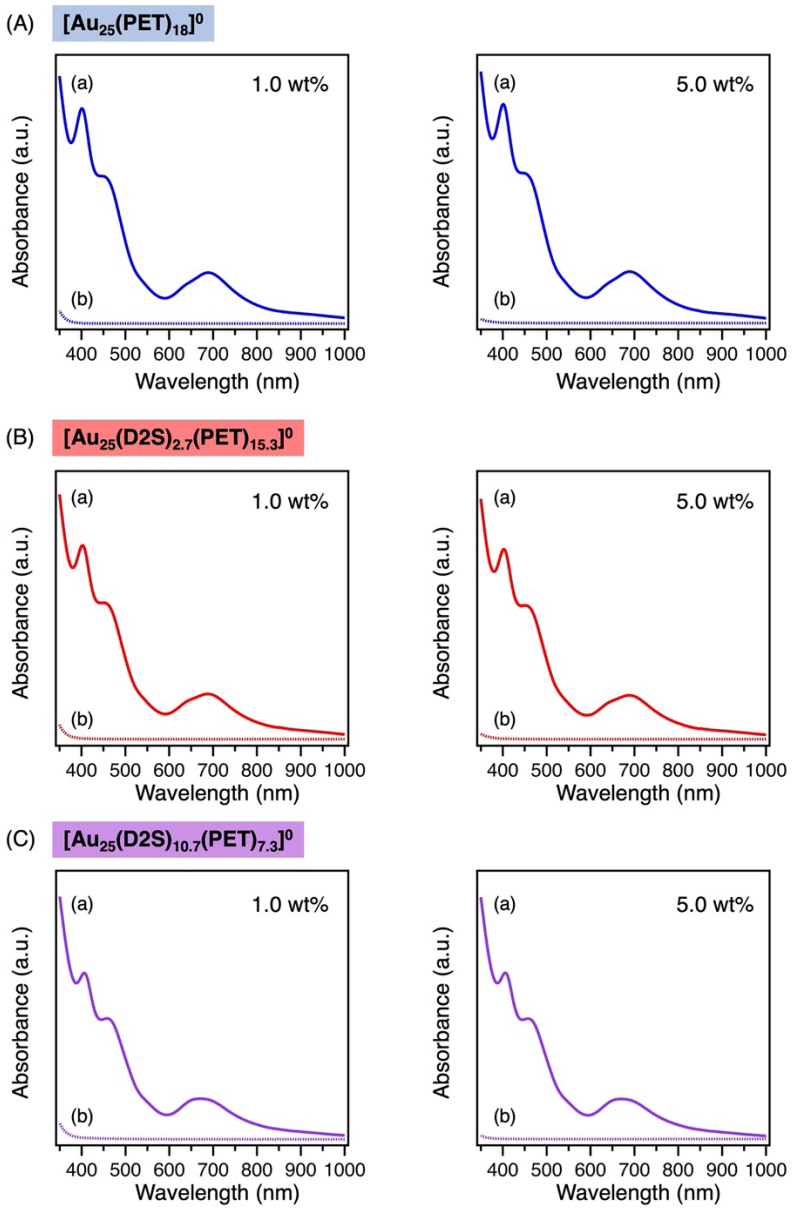

Figure S4. UV-vis absorption spectra of $[Au_{25}(D2S)_x(PET)_{18-x}]^0$ with x = (A) 0, (B) 2.7, and (C) 10.7, (a) before and (b) after adsorption onto the carbon support. The loading amount was 1.0 and 5.0 wt% for left and right columns, respectively.

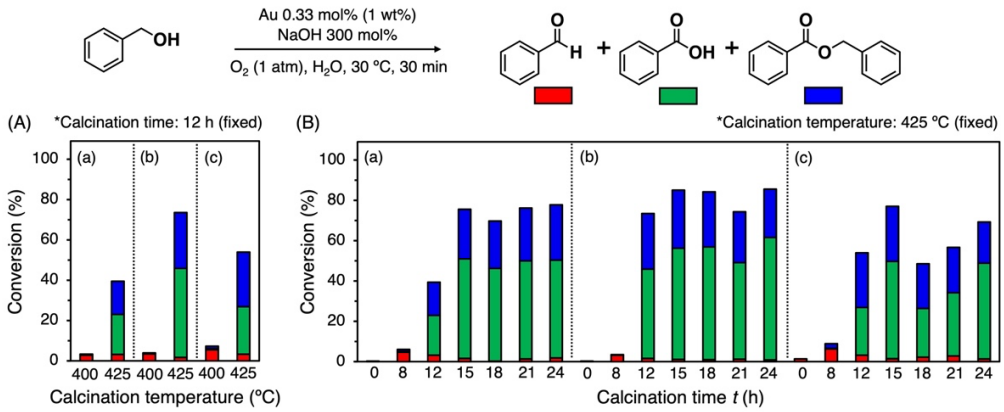

Figure S5. Catalytic activity in benzyl alcohol oxidation over 1.0-$Au_{25}(D2S)_x$/C with x = (a) 0, (b) 2.7, and (c) 10.7, respectively, calcined at various (A) temperatures and (B) times.

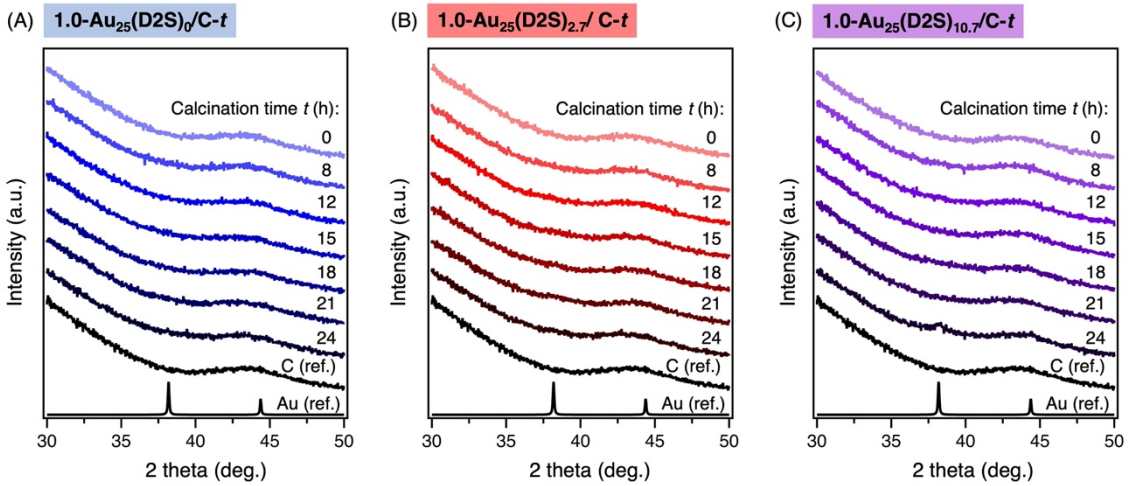

Figure S6. PXRD patterns of 1.0-$Au_{25}(D2S)_x$/C-t with x = (A) 0, (B) 2.7, and (C) 10.7, respectively, calcined at 425 °C. C (ref.) corresponds to pristine carbon support without calcination.

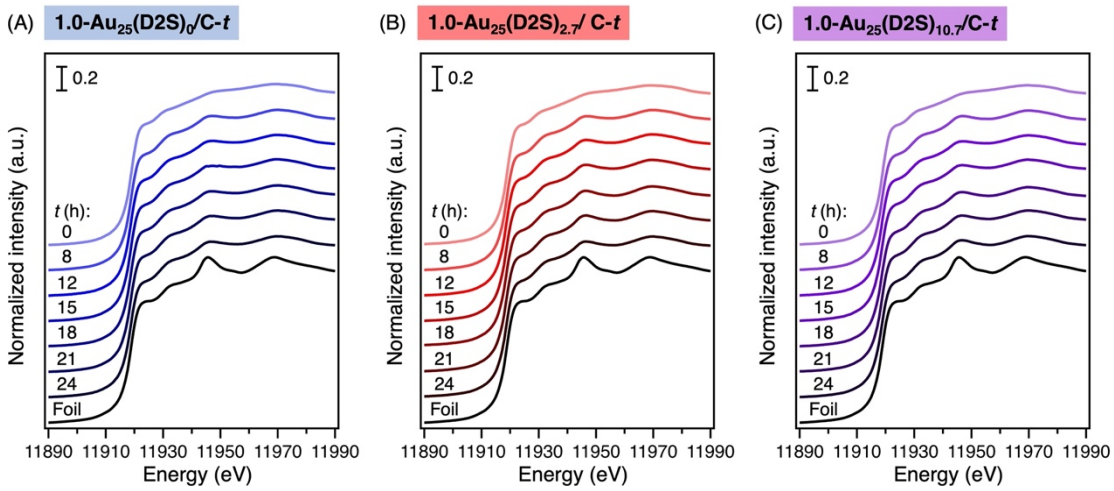

Figure S7. Au L_3-edge XANES spectra of 1.0-$Au_{25}(D2S)_x$/C-t with x = (A) 0, (B) 2.7, and (C) 10.7, respectively, calcined at 425 °C.

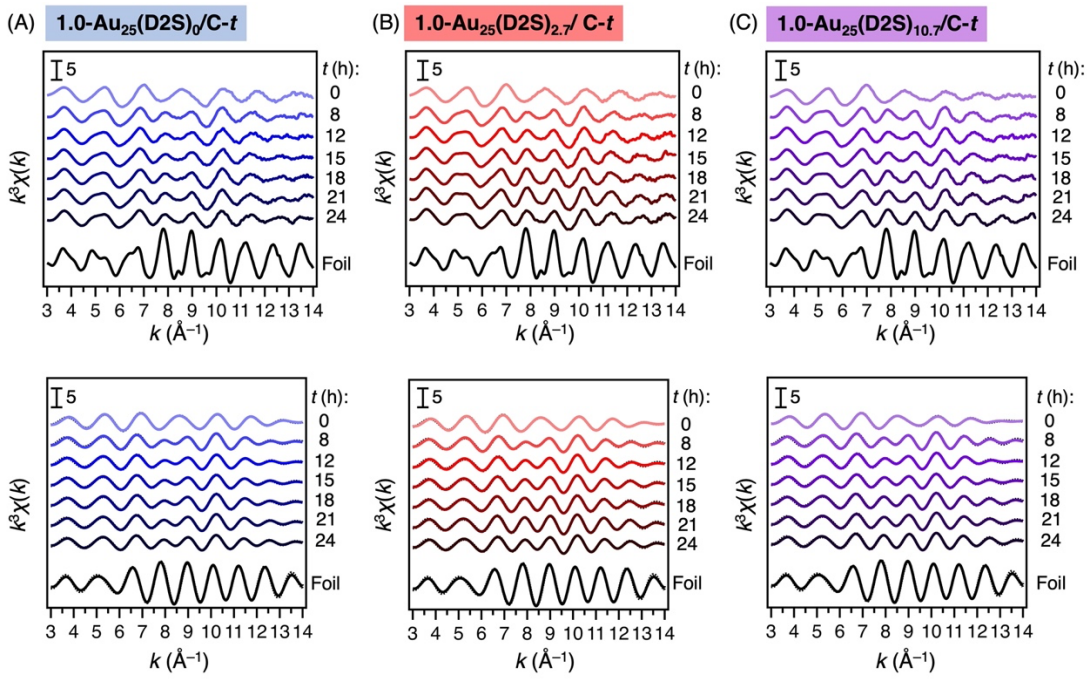

Figure S8. Au L_3-edge EXAFS oscillations (top) and corresponding fitting curves of EXAFS oscillation in *k*-space (bottom) of 1.0-$Au_{25}(D2S)_x$/C-*t* with *x* = (A) 0, (B) 2.7, and (C) 10.7, respectively, calcined at 425 °C. Solid and dotted lines in bottom panels represent raw data and the fitting, respectively.

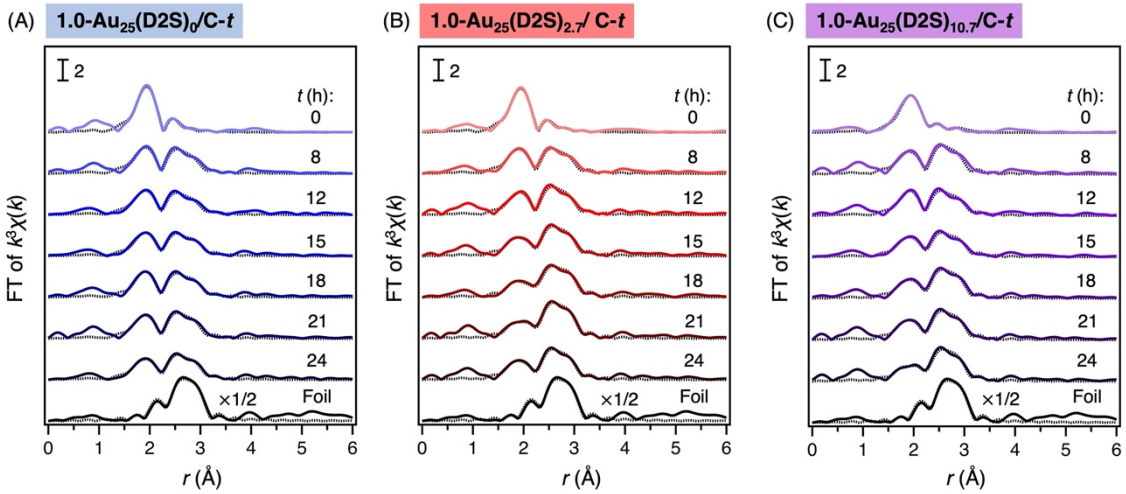

Figure S9. Au L_3-edge FT-EXAFS spectra of 1.0-$Au_{25}(D2S)_x$/C-*t* with *x* = (A) 0, (B) 2.7, and (C) 10.7, respectively, calcined at 425 °C. The intensity of Au foil was halved for clarity. Solid and dotted lines represent raw data and the fitting, respectively.

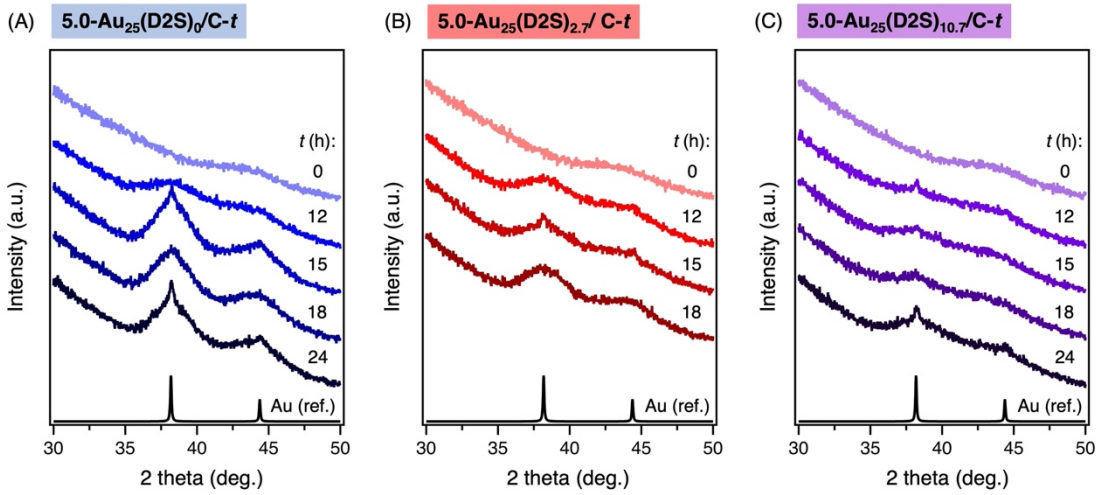

Figure S10. PXRD patterns of 5.0-$Au_{25}(D2S)_x$/C-*t* with *x* = (A) 0, (B) 2.7, and (C) 10.7, respectively, calcined at 425 °C.

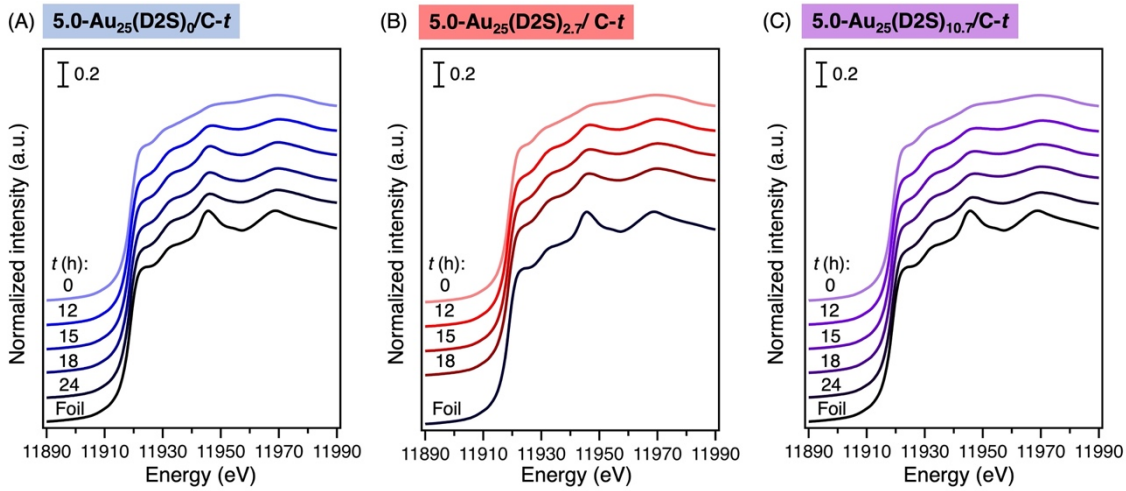

Figure S11. Au L_3-edge XANES spectra of 5.0-$Au_{25}(D2S)_x$/C-*t* with *x* = (A) 0, (B) 2.7, and (C) 10.7, respectively, calcined at 425 °C.

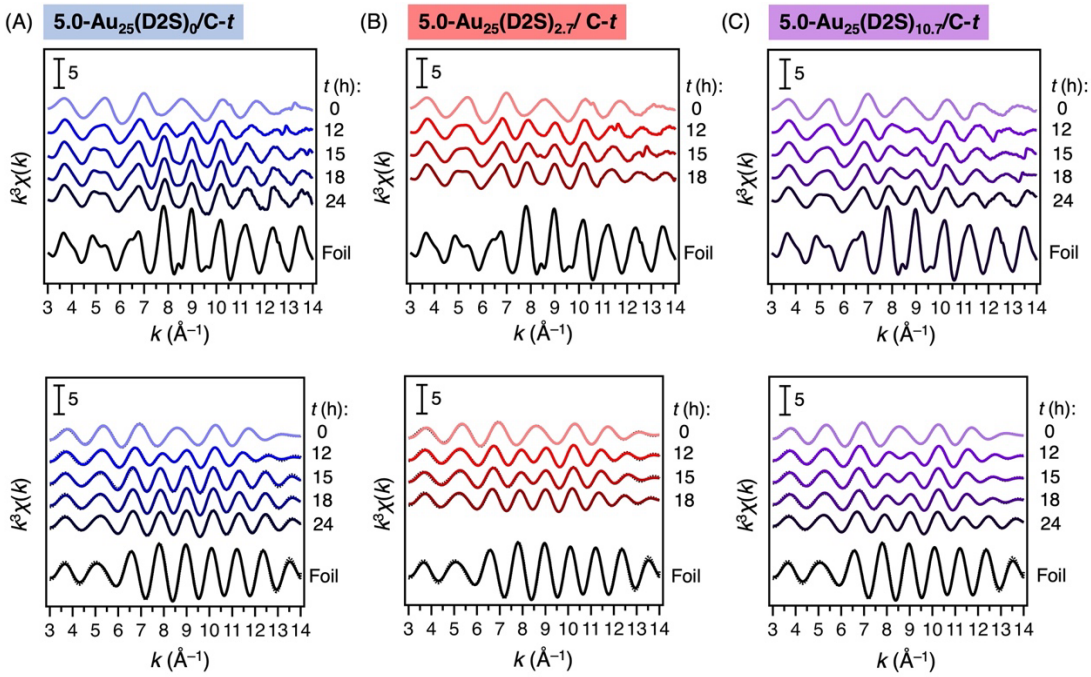

Figure S12. Au L_3-edge EXAFS oscillations (top) and corresponding fitting curves of EXAFS oscillation in *k*-space (bottom) of 5.0-$Au_{25}(D2S)_x$/C-*t* with *x* = (A) 0, (B) 2.7, and (C) 10.7, respectively, calcined at 425 °C. Solid and dotted lines in bottom panels represent the raw data and the fitted results, respectively.

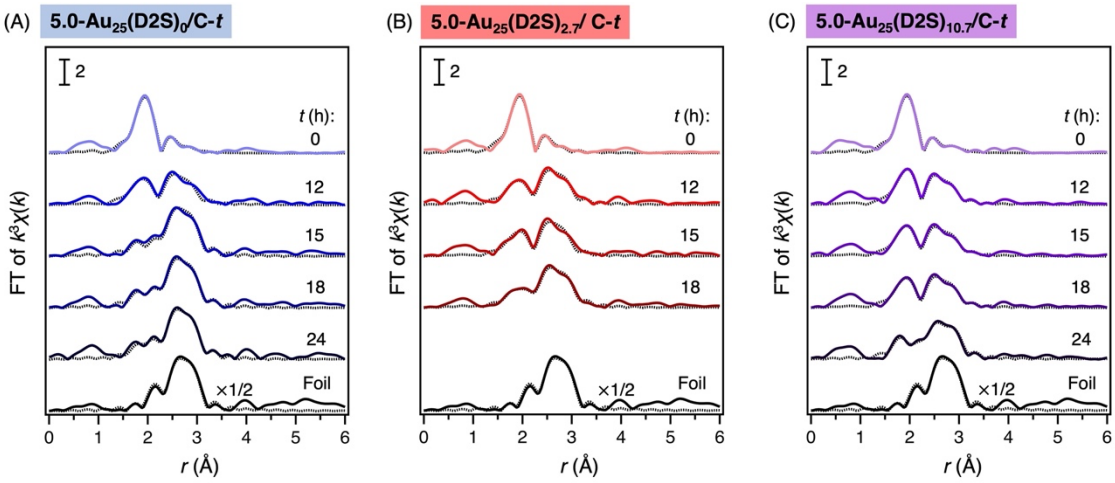

Figure S13. Au L_3-edge FT-EXAFS spectra of 5.0-$Au_{25}(D2S)_x$/C-*t* with *x* = (A) 0, (B) 2.7, and (C) 10.7, respectively, calcined at 425 °C. The intensity of Au foil was halved for clarity. Solid and dotted lines represent the raw data and the fitted results, respectively.

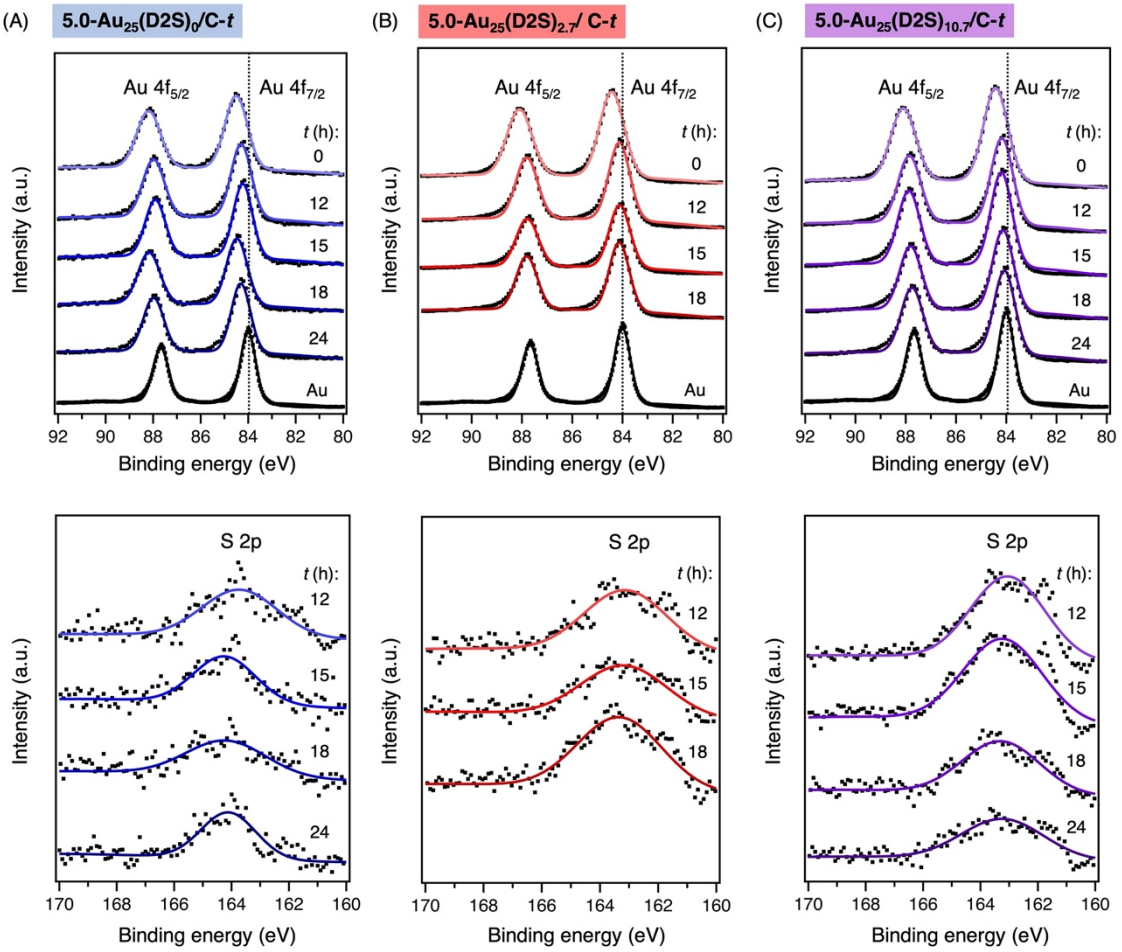

Figure S14. Au 4f (top) and S 2p (bottom) of XP spectra of 5.0-$Au_{25}(D2S)_x$/C-*t* with *x* = (A) 0, (B) 2.7, and (C) 10.7, respectively, calcined at 425 °C. Dots and solid lines correspond to the raw data and fitted results, respectively. Intensity is changed for clarity.

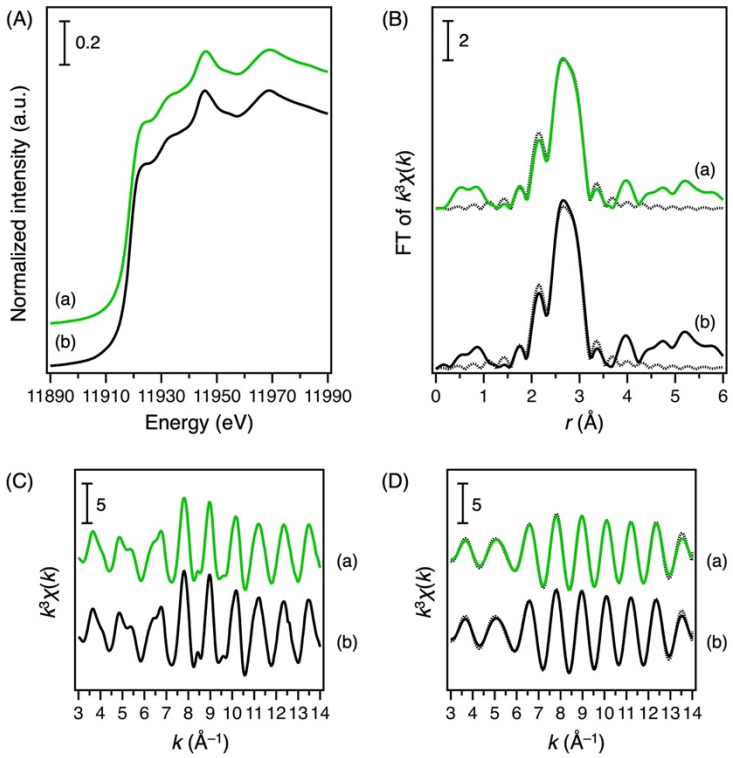

Figure S15. Au L_3-edge (A) XANES, (B) FT-EXAFS, (C)EXAFS oscillations, and (D) fitting curves of EXAFS oscillation in *k*-space of (a) 5.0-AuNP/C and (b) Au foil. Solid and dotted lines in (B) and (D) represent the raw data and the fitted results, respectively.

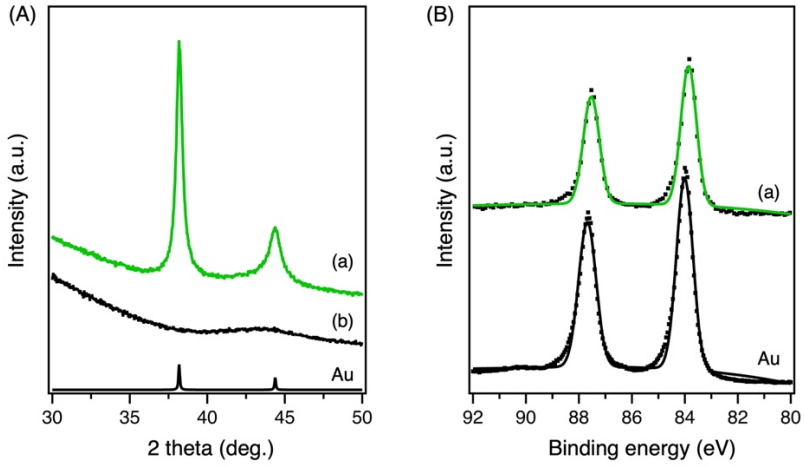

Figure S16. (A) PXRD patterns of (a) 5.0-AuNP/C and (b) pristine carbon support. (B) Au 4f XP spectra of (a) 5.0-AuNP/C. Dots and solid lines correspond to the raw data and fitted results, respectively.

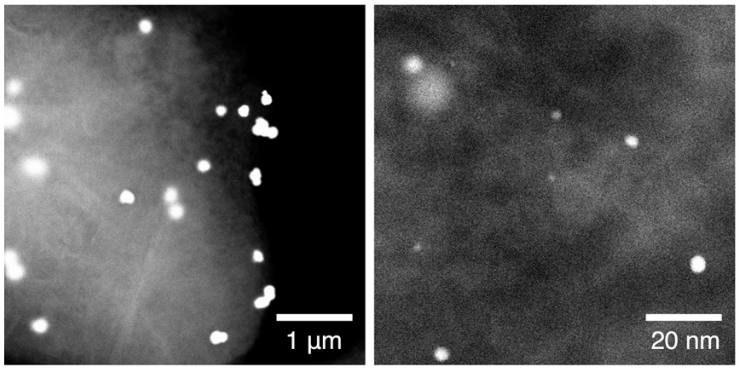

Figure S17. Typical AC-HAADF-STEM images of 5.0-AuNP/C.

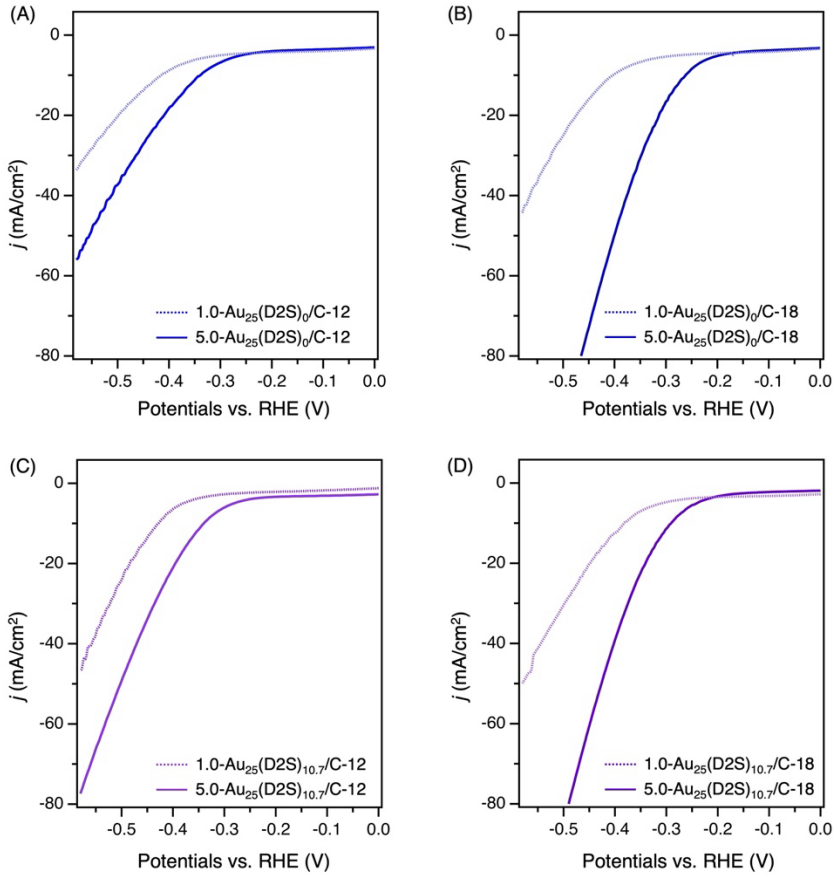

Figure S18. LSV curves for (A) $Au_{25}(D2S)_0$/C-12, (B) $Au_{25}(D2S)_0$/C-18, (C) $Au_{25}(D2S)_{10.7}$/C-12 and (D) $Au_{25}(D2S)_{10.7}$/C-18. The solid and dotted lines represent the data for the catalysts with the loading amount of 5.0 and 1.0 wt%, respectively.

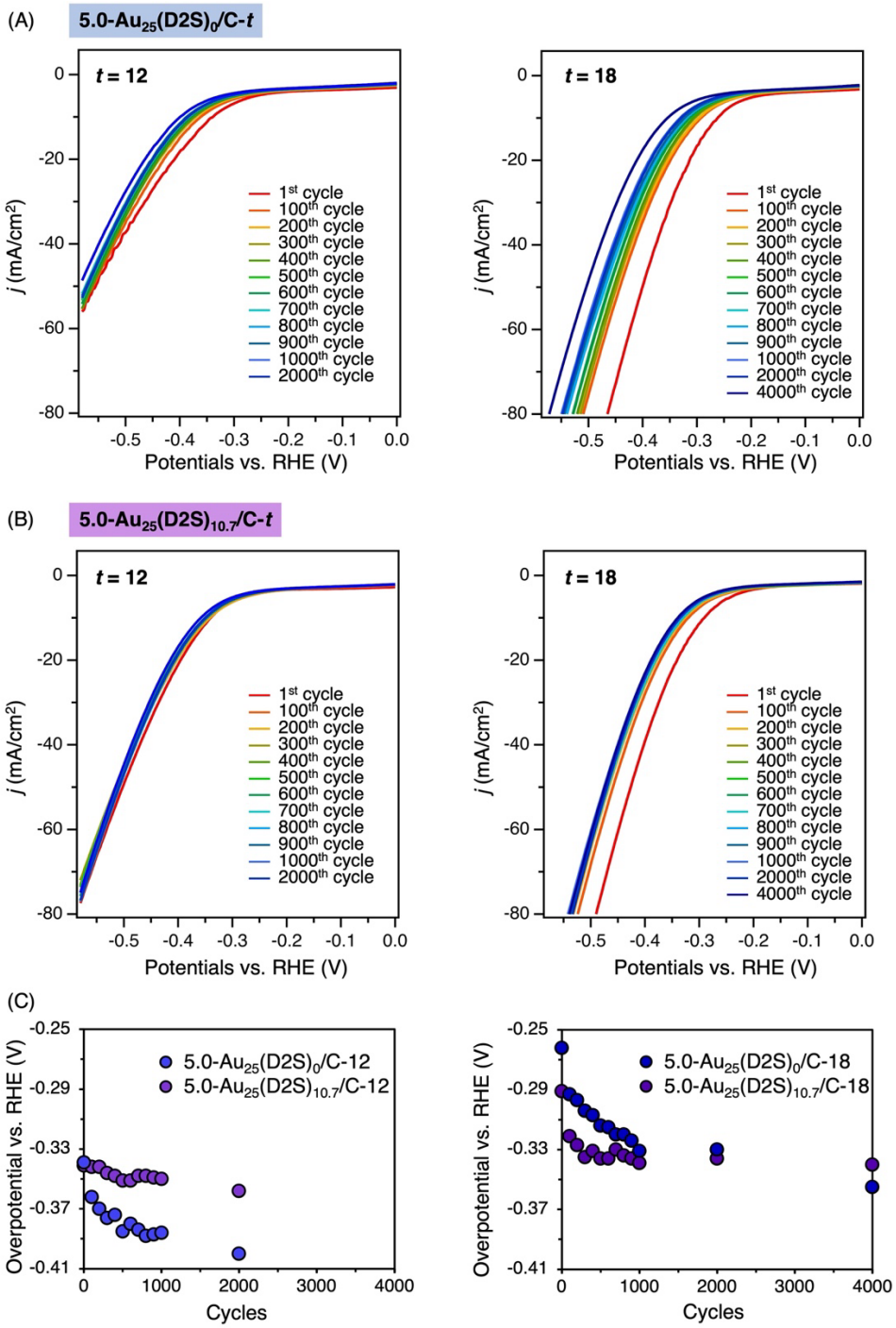

Figure S19. LSV curves of (A) 5.0-$Au_{25}(D2S)_0$/C-*t* and (B) 5.0-$Au_{25}(D2S)_{10.7}$/C-*t* with *t* = 12 (left) and 18 (right) after sweeping several cycles by cyclic voltammetry. (C) Changes of overpotentials η (vs. RHE) during the sweeping by cyclic voltammetry.

Table S1. Structural parameters obtained by curve-fitting analysis of EXAFS in Fig. S8.

Sample	*t* [a]	Bond	CNs [b]	*r* (Å) [c]	DW (Å^2) [d]	R(%) [e]
1.0-$Au_{25}(D2S)_0$/C-*t*	0	Au–Au	0.8(6)	2.71(3)	0.0076(68)	6.1
		Au–S	1.6(2)	2.32(1)	0.0055(18)	
	8	Au–Au	4.5(9)	2.78(1)	0.0108(23)	11.8
		Au–S	1.2(2)	2.33(1)	0.0066(24)	
	12	Au–Au	4.4(9)	2.78(1)	0.0112(23)	10.2
		Au–S	1.0(2)	2.33(1)	0.0066(24)	
	15	Au–Au	4.5(8)	2.79(1)	0.0110(21)	7.9
		Au–S	0.9(1)	2.33(1)	0.0058(24)	
	18	Au–Au	4.4(8)	2.79(1)	0.0106(21)	8.9
		Au–S	0.9(1)	2.33(1)	0.0050(21)	
	21	Au–Au	4.7(8)	2.79(1)	0.0106(21)	8.4
		Au–S	0.9(2)	2.33(1)	0.0055(27)	
	24	Au–Au	4.8(8)	2.80(1)	0.0108(19)	7.3
		Au–S	0.9(2)	2.33(1)	0.0066(31)	
1.0-$Au_{25}(D2S)_{2.7}$/C-*t*	0	Au–Au	0.7(5)	2.73(4)	0.0071(67)	4.8
		Au–S	1.6(2)	2.32(1)	0.0059(18)	
	8	Au–Au	4.1(2)	2.79(1)	0.0100(20)	10.3
		Au–S	1.1(2)	2.33(1)	0.0069(25)	
	12	Au–Au	4.9(9)	2.79(1)	0.0102(20)	12.0
		Au–S	0.9(2)	2.34(1)	0.0058(27)	
	15	Au–Au	5.4(9)	2.81(1)	0.0104(18)	8.7
		Au–S	0.7(2)	2.34(1)	0.0059(35)	
	18	Au–Au	5.6(3)	2.81(1)	0.0102(18)	12.6
		Au–S	0.7(1)	2.33(2)	0.0071(45)	
	21	Au–Au	5.5(3)	2.81(1)	0.0094(17)	12.2
		Au–S	0.7(2)	2.34(2)	0.0066(47)	
	24	Au–Au	5.5(9)	2.81(1)	0.0104(18)	8.2
		Au–S	0.8(2)	2.34(1)	0.0058(35)	
1.0-$Au_{25}(D2S)_{10.7}$/C-*t*	0	Au–Au	1.3(7)	2.77(3)	0.0114(66)	4.7
		Au–S	1.5(1)	2.32(1)	0.0072(19)	
	8	Au–Au	4.3(2)	2.79(1)	0.0096(20)	13.6
		Au–S	1.0(2)	2.33(1)	0.0067(28)	
	12	Au–Au	4.5(3)	2.79(1)	0.0106(21)	11.7
		Au–S	0.8(2)	2.33(1)	0.0050(26)	
	15	Au–Au	4.3(2)	2.80(1)	0.0104(18)	11.7
		Au–S	0.8(1)	2.33(1)	0.0066(31)	

	18	Au–Au	4.9(2)	2.80(1)	0.0100(18)	10.7
		Au–S	0.8(2)	2.34(1)	0.0062(35)	
	21	Au–Au	5.1(8)	2.79(1)	0.0104(18)	10.0
		Au–S	0.8(2)	2.33(1)	0.0066(34)	
	24	Au–Au	5.0(2)	2.79(1)	0.0094(17)	14.8
		Au–S	0.7(1)	2.33(2)	0.0076(50)	
Au foil		Au–Au	11.8(1.3)	2.85(1)	0.0086(11)	8.8

[a] Calcination time (h). Sample with t = 0 corresponds to those without calcination. [b] Coordination number. [c] Bond length. [d] Debye-Waller factor. [e] $R = (\sum(k^3\chi^{data}(k) - k^3\chi^{fit}(k))^2)^{1/2}/(\sum(k^3\chi^{data}(k))^2)^{1/2}$. Standard deviation values are shown in parentheses.

Table S2. Structural parameters obtained by curve-fitting analysis of EXAFS in Figs. S12 and S15.

Sample	*t* [a]	Bond	CNs [b]	*r* (Å) [c]	DW (Å^2) [d]	R(%) [e]
5.0-$Au_{25}(D2S)_0$/C-*t*	0	Au–Au	1.0(6)	2.75(3)	0.0081(59)	5.0
		Au–S	1.5(2)	2.32(1)	0.0050(17)	
	12	Au–Au	4.8(3)	2.78(1)	0.0110(21)	13.6
		Au–S	1.0(2)	2.33(1)	0.0076(30)	
	15	Au–Au	7.1(3)	2.82(1)	0.0102(12)	11.9
		Au–S	0.6(1)	2.33(1)	0.0086(15)	
	18	Au–Au	7.3(1.0)	2.82(1)	0.0102(16)	7.7
		Au–S	0.6(1)	2.34(2)	0.0081(63)	
	24	Au–Au	7.6(4)	2.82(1)	0.0104(16)	7.6
		Au–S	0.6(1)	2.36(2)	0.0072(61)	
5.0-$Au_{25}(D2S)_{2.7}$/C-*t*	0	Au–Au	0.7(5)	2.71(4)	0.0067(62)	6.3
		Au–S	1.5(2)	2.32(1)	0.0053(19)	
	12	Au–Au	5.0(3)	2.79(1)	0.0104(18)	11.1
		Au–S	0.8(2)	2.33(1)	0.0062(35)	
	15	Au–Au	5.3(9)	2.79(1)	0.0108(20)	14.1
		Au–S	0.8(1)	2.35(1)	0.0058(29)	
	18	Au–Au	7.4(1.2)	2.81(1)	0.0114(19)	8.8
		Au–S	0.7(3)	2.35(2)	0.0072(54)	
5.0-$Au_{25}(D2S)_{10.7}$/C-*t*	0	Au–Au	1.1(6)	2.77(3)	0.0090(59)	2.6
		Au–S	1.4(2)	2.32(1)	0.0046(15)	
	12	Au–Au	3.4(7)	2.77(1)	0.0098(22)	7.3
		Au–S	0.9(2)	2.33(1)	0.0050(24)	
	15	Au–Au	4.6(8)	2.78(1)	0.0110(21)	9.5
		Au–S	0.8(2)	2.33(1)	0.0055(27)	
	18	Au–Au	4.4(8)	2.78(1)	0.0104(20)	9.1
		Au–S	0.8(2)	2.33(1)	0.0052(27)	
	24	Au–Au	5.9(8)	2.82(1)	0.0106(14)	6.0
		Au–S	0.5(1)	2.29(2)	0.0052(40)	
5.0-AuNP/C		Au–Au	10.1(1.1)	2.85(1)	0.0090(11)	10.8
Au foil		Au–Au	11.8(1.3)	2.85(1)	0.0086(11)	8.8

[a] Calcination time (h). Sample with *t* = 0 corresponds to those without calcination. [b] Coordination number. [c] Bond length. [d] Debye-Waller factor. [e] $R = (\sum(k^3\chi^{data}(k) - k^3\chi^{fit}(k))^2)^{1/2}/(\sum(k^3\chi^{data}(k))^2)^{1/2}$. Standard deviation values are shown in parentheses.

Table S3. Comparison of the catalytic activity of electrocatalytic HER catalyzed by Au_{25} clusters.

Entry	Catalyst	η (V) [a]	Current density (mA cm^{-2})	Electrolyte	Ref.
1	5.0-$Au_{25}(D2S)_0$/C-0	–0.53	7.9 (–0.5 V vs. RHE)	0.5M H_2SO_4	This work
2	5.0-$Au_{25}(D2S)_0$/C-12	–0.34	35.0 (–0.5 V vs. RHE)		
3	5.0-$Au_{25}(D2S)_0$/C-18	–0.27	98.0 (–0.5 V vs. RHE)		
4	5.0-$Au_{25}(D2S)_{10.7}$/C-0	–0.59	4.9 (–0.5 V vs. RHE)		
5	5.0-$Au_{25}(D2S)_{10.7}$/C-12	–0.34	49.3 (–0.5 V vs. RHE)		
6	5.0-$Au_{25}(D2S)_{10.7}$/C-18	–0.29	85.0 (–0.5 V vs. RHE)		
7 [b]	$[Au_{25}(SC6)_{18}]^0$/C	–	4.2 (–0.6 V vs. RHE)	1.0M Britton-Robinson buffer solution and 2.0M KCl (pH 3)	S5
8 [c]	$[Au_{25}(PET)_{18}]^0$/C	–0.56	3.0 (–0.5 V vs. RHE)	0.5M H_2SO_4	S6
9 [c]	$[Au_{25}(PET)_{18}]^0$	–	3.9 (–0.5 V vs. RHE)	0.2M $HClO_4$ (pH 7)	S7
10 [d]	$[Au_{25}(SC12)_{18}]^0$	–	0.4 (–0.5 V vs. RHE)		
11 [c]	$[Au_{25}(PET)_{18}]^-$	–	8.1 (–0.5 V vs. RHE)		
12 [c]	$[Au_{25}(PET)_{18}]^-$	–	5.1 (–0.3 V vs. RHE)	0.5M H_2SO_4	S8

[a] Overpotential at 10 mA cm^{-2}. [b] SC6: *n*-hexanethiolate. [c] PET: 2-phenylethanethiolate. [d] SC12: *n*-dodecanethiolate.

References

S1. C. A. Schneider, W. S. Rasband and K. W. Eliceiri, *Nat. Methods*, 2012, **9**, 671–675.

S2. T. Omoda, S. Takano, S. Masuda and T. Tsukuda, *Chem. Commun.*, 2021, **57**, 12159–12162.

S3. S. Masuda, S. Takano, S. Yamazoe and T. Tsukuda, *Nanoscale*, 2022, **14**, 3031–3039.

S4. K. Sakamoto, S. Masuda, S. Takano and T. Tsukuda, *ACS Catal.*, 2023, **13**, 3263–3271.

S5. W. Choi, G. Hu, K. Kwak, M. Kim, D. Jiang, J.-P. Choi, and D. Lee, *ACS Appl. Mater. Interfaces*, 2018, **10**, 44645–44653.

S6. X. Li, S. Takano, and T. Tsukuda, *J. Phys. Chem. C*, 2021, **125**, 23226–23230.

S7. B. Kumar, T. Kawawaki, N. Shimizu, Y. Imai, D. Suzuki, S. Hossain, L. V. Nair, and Y. Negishi, *Nanoscale*, 2020, **12**, 9969–9979.

S8. Y. Li, S. Li, A. V. Nagarajan, Z. Liu, S. Nevins, Y. Song, G. Mpourmpakis, and R. Jin, *J. Am. Chem. Soc.*, 2021, **143**, 11102–11108.